



Explosive expansion of a slowly decompressed magma analogue: Evidence for delayed bubble nucleation

Eleonora Rivalta

GFZ GeoForschungsZentrum, Section 2.1, Physics of Earthquakes and Volcanoes, Telegrafenberg, DE-14473, Potsdam, Germany (rivalta@gfz-potsdam.de)

School of Earth and Environment, University of Leeds, Leeds, UK

Institute of Geophysics, University of Hamburg, Hamburg, Germany

Karen Pascal

School of Earth and Environment, University of Leeds, Leeds, UK

Jeremy Phillips

School of Earth Sciences, University of Bristol, Bristol, UK

Alessandro Bonaccorso

INGV, Sezione di Catania, Piazza Roma 2, Catania, Italy

[1] While ascending in the plumbing system of volcanoes, magma undergoes decompression at rates spanning several orders of magnitude and set by a number of factors internal and external to the volcano. Slow decompression generally results in an effusive or mildly explosive expansion of the magma, but counterexamples of sudden switches from effusive to explosive eruptive behavior have been documented at various volcanoes worldwide. The mechanisms involved in this behavior are currently debated, in particular for basaltic magmas. Here, we explore the interplay between decompression rate and vesiculation vigor by decompressing a magma analogue obtained by dissolving pine resin into acetone in varying proportions. Analogue experiments allow direct observations of the processes of bubble nucleation and growth, flow dynamics, and fragmentation that is not currently possible with magmatic systems. Our mixtures contain solid particles, and upon decompression, nucleation of acetone bubbles is observed. We find that mixtures with a high acetone content, containing smaller and fewer solid particles, experience strong supersaturation and fragment under very slow decompressions, despite having low viscosity, while mixtures with lower acetone content, with more and larger solid particles, degas efficiently without fragmentation. We interpret our results in terms of delayed bubble nucleation due to a lack of efficient nucleation sites. We discuss how a similar mechanism might induce violent, explosive expansion in volatile-rich and poorly crystalline low-silica magmas, by analogy with the behavior of rhyolitic magmas.

Components: 11,253 words, 7 figures, 1 table.

Keywords: magma fragmentation; basaltic magma; analogue laboratory experiments; slow decompression; bubble nucleation; explosive volcanic eruptions.

Index Terms: 8428 Explosive volcanism: Volcanology; 8434 Magma migration and fragmentation: Volcanology; 8414 Eruption mechanisms and flow emplacement: Volcanology; 8439 Physics and chemistry of magma bodies: Volcanology; 8445 Experimental volcanism: Volcanology; 4302 Geological: Natural Hazards.



Received 27 February 2013; Revised 20 May 2013; Accepted 22 May 2013; Published 00 Month 2013.

Rivalta, E., K. Pascal, J. Phillips, and A. Bonaccorso (2013), Explosive expansion of a slowly decompressed magma analogue: Evidence for delayed bubble nucleation, *Geochem. Geophys. Geosyst.*, 14, doi:10.1002/ggge.20183.

1. Introduction

[2] Sudden decompression of magma, induced for example by the removal of mass from a volcanic edifice (flank collapse, landslides, glacier melting, lake drainage), has the potential to cause explosive eruptions, depending on the amount of decompression and the volatile content of magma. A link between explosive high-silica volcanism and slow decompression of magma (e.g., induced by effusive activity) has also been suggested by decompression experiments on rhyolite [Cashman *et al.*, 2000; Castro and Gardner, 2008]. The established physical explanation of slow decompression as a trigger for explosive eruptions is “viscous restraint”: the induced expansion of gas bubbles might be resisted by high viscous stresses in very viscous magmas to such an extent that enough pressure builds up within the bubbles to eventually rupture their walls, resulting in explosive expansion. Additionally, laboratory experiments have suggested that high-silica explosive eruptions during slow decompression might also exhibit “delayed bubble nucleation” [Sparks, 1978; Mangan and Sisson, 2000; Mourtada-Bonnefoi and Laporte, 2002; Pinkerton *et al.*, 2002; Mangan *et al.*, 2004; Mangan and Sisson, 2005]: the nucleation of gas bubbles during decompression may be retarded in poorly crystalline magmas by a lack of efficient nucleation sites and slow volatile diffusivity, so that the magma becomes progressively supersaturated and eventually expands explosively once a supersaturation threshold is reached and bulk vesiculation is triggered. Hurwitz and Navon [1994] studied the efficiency of different types of crystals in facilitating gas exsolution in rhyolitic magma. They found that Fe-Ti oxides are very efficient sites of nucleation, and their presence favors equilibrium degassing during decompression. On the contrary, magma with a low crystal content or containing crystals that are inefficient as nucleation sites, such as feldspar or quartz, requires large supersaturation to nucleate bubbles.

[3] Low-silica magmas can also erupt explosively. While a large majority of basaltic vol-

canic eruptions are effusive or mildly explosive, as in Strombolian or Hawaiian activity [Vergnoille and Mangan, 2000], basaltic volcanoes switch occasionally to explosive activity of greater intensity, up to Plinian, sometimes with little warning [Williams and Self, 1983; Walker *et al.*, 1984; Coltelli *et al.*, 1998; Doubik and Hill, 1999; Gurenko *et al.*, 2005; Höskuldsson *et al.*, 2007]. Significant effort has been made in the last few years to understand violent explosive basaltic eruptions, investigating the eruption products [Polacci *et al.*, 2001, 2003; Gurioli *et al.*, 2008; Sable *et al.*, 2009] and how the physical properties of low-silica magmas change with volatile content [Polacci *et al.*, 2006; Larsen, 2008; Métrich *et al.*, 2009]. The physics of the expansion and fragmentation of bubbly, low-viscosity fluids upon decompression is still poorly understood; this has motivated experimental analogue studies [Namiki and Manga, 2005, 2006, 2008] investigating the style of expansion of bubbly fluids as a function of amount of decompression, decompression rate, and conduit and magma parameters. Besides describing the phenomenology of the various expansion styles as function of vesicularity and decompression rate, those studies offer a quantitative physical model based on rates of bubbly liquid deformation for how sudden decompression may lead to the fragmentation of bubbly low-viscosity magma.

[4] The mechanisms by which slowly decompressed basaltic magmas can erupt explosively remain unclear. Decompression rates of the order of 100–400 Pa s⁻¹, typical of lava effusion, are not commonly assumed to be potentially hazardous: lava effusion, particularly at basaltic volcanoes, is considered a low-risk eruptive style, and the few laboratory experiments investigating the link between slow decompression and explosivity found that significantly higher rates were needed to observe fragmentation. Namiki and Manga [2006] decompressed at various rates bubbly fluids and observed fragmentation only for

decompression rates larger than about 0.5–1 MPa s⁻¹; Stix and Phillips [2012] obtained similar results for a set of volatile-bearing gum rosin and acetone mixtures. However, counterexamples of slowly decompressed basaltic systems that underwent violent explosive eruptions have been documented. Switches in the eruptive style in the sequence: Strombolian → effusive → high-energy explosive → effusive have been inferred, for example, for the ~2000 BP eruption at Xitle volcano in the central Trans-Mexican Volcanic Belt [Cervantes and Wallace, 2003]. They have also been observed at Stromboli volcano in 2003 and 2007 [Calvari et al., 2011] in the following sequence. Lava effusion started from fissures that opened a few hundred meters below the summit, while the usual low-energy explosive activity ceased; lava effusion persisted for a few weeks, then suddenly an explosive paroxysmal event of unusual energy (a 1 km sized eruption column) occurred, transporting to the surface magma with low crystallinity and high volatile content from a deep reservoir, not tapped during normal Strombolian activity. Such switches in erupting behavior are still unexplained. For the eruption at Xitle, it has been suggested that a recharge event induced a sudden increase of magma overpressure in the conduit and an increased magma ascent rate [Cervantes and Wallace, 2003]. This mechanism is not fully satisfactory, at least for Stromboli, as lava flow certainly induced an increased ascent rate, but the lava flow rate was highest in the initial phase of the effusion, and it subsequently decreased systematically and significantly, and was about an order of magnitude lower on the day of the paroxysm [Calvari et al., 2011]. Magma partitioning and simultaneous eruption of gas-rich magma from the vent and of gas-poor magma from a fissure at the base of the cinder cone, proposed by Krauskopf [1948] for Paricutin volcano, has also been suggested by Cervantes and Wallace [2003] for Xitle. Although at Stromboli the lava was flowing from fissures located a few hundred meters below the summit craters, a partition mechanism can be excluded for the 2003 and 2007 paroxysms at Stromboli, as the Strombolian activity at the summit vents had stopped completely during lava effusion.

[5] A few studies have offered physical mechanisms for mild to intermediate explosive expansion styles at low-silica volcanoes. Namiki and Manga [2008] suggest that the stretching of the bubbly column of magma in the conduit during

decompression-induced expansion (or “inertial fragmentation”) might explain explosive basaltic eruptions during slow decompression. Other existing conceptual models [Vergnolle and Jaupart, 1986; Parfitt and Wilson, 1995; Namiki and Manga, 2006] explain the generation of Hawaiian sustained lava fountaining and mild to intermediate isolated Strombolian explosions [Aiuppa et al., 2011]. However, it is difficult to apply any of them, for example, to explain basaltic Plinian eruptions or to sudden switches from effusive to explosive eruptive styles. Some authors suggest that the kinetics of bubble or crystal nucleation [Sable et al., 2006; Houghton and Gonnermann, 2008; Sable et al., 2009], or the dynamics of degassing [Schipper et al., 2010], may play a dominant role in explosive eruptions of basaltic magma, and indeed in supersaturated magmas, large quantities of energy are stored in a metastable equilibrium and can be released over short time scales. However, a conceptual model of high-energy explosive eruptions at basaltic volcanoes is still missing, and the fine-scale mechanisms able to cause the fragmentation of low-viscosity magma without any sudden decompression are poorly understood.

[6] We present here laboratory observations of the interplay between decompression and vesiculation rates from fast and slow decompression experiments using a magma analogue containing dissolved volatiles and solid particles. As expected, we observe that all mixtures fragment during sudden decompression, but some vesiculate violently and fragment during decompressions as slow as 50–400 Pa s⁻¹. Based on our observations, supported by elements of nucleation theory and published petrological laboratory experiments, we propose that slow decompression might induce strong supersaturation and potential explosivity in basaltic magma if bubble nucleation is delayed by lack of crystals to act as nuclei or by general inefficiency of nucleation, as has been proposed for rhyolitic magmas. Our experimental observations support the idea that delayed nucleation may turn slow decompression of magma (e.g., induced in the conduit by lava effusion) into potential explosive behavior, provided the crystallinity of the magma is poor or inefficient as an adjuvant for bubble nucleation. Our experiments suggest a possible large-scale model for delayed bubble nucleation as a mechanism potentially leading to violent explosive eruptions at low-silica volcanoes, that we speculatively apply to the 2003 and 2007 paroxysms at Stromboli.

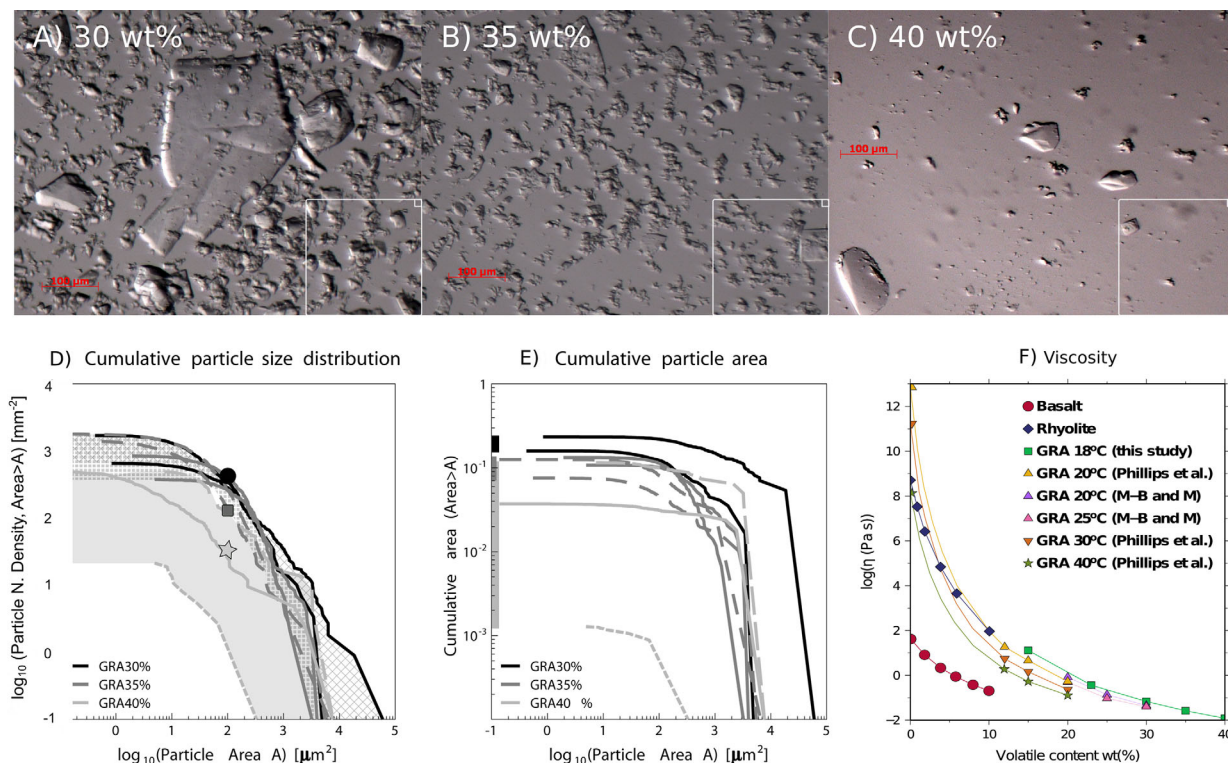


Figure 1. (a–c) Optical microscope image of a droplet of 30, 35 and 40 wt % acetone GRA mixtures. The average dimension and number density of the solid particles contained in the mixtures anticorrelate with acetone content. See Table 1 for the physical properties of the mixtures and for an estimate of their crystallinity estimated in the square regions of the images bordered in white. (d) Particle size distribution for eight samples with acetone concentration 30, 35 or 40 wt %. The size distribution is approximately a power law across all acetone concentrations. The uncertainty on the number of particles is low for high acetone concentration (40 wt %) and much larger for low acetone concentration (30 wt %), for which it is underestimated, in particular, for small size particles, as overlapping particles were neglected. (e) Cumulative area covered by the particles for the same image area. The cumulative area is increasingly underestimated for lower acetone concentrations (or higher particle content) as overlapping particles were counted only once. (f) Viscosity of GRA mixtures as a function of acetone content for 18, 20, 25, 30, and 40°C. The data are from this study (Table 1), from Phillips *et al.* [1997] and from Mourtada-Bonnefoi and Mader [2004]. For comparison, the viscosity variation of basalt at 1200°C and rhyolite at 850°C as a function of water content are shown [Shaw, 1972]. Data from Phillips *et al.* [1995].

2. Experimental Methods

2.1. Magma Analogue

[7] Gum rosin-acetone (GRA) mixtures of different initial acetone concentration (here 15–40 wt % acetone in gum rosin) were used as magma analogues, being prepared by solving brittle gum rosin blocks [Fiebach and Grimm, 2000] into acetone in a continuously stirred and sealed glass flask for about 24 h. Macroscopically, GRA mixtures appear purely liquid, although occasionally we visually observed solid gum rosin particles in mixtures of lower acetone concentration (<30 wt %). However, optical microscope images (Figures 1a–c for pictures of droplets of 30, 35, and 40 wt %,

GRA mixtures respectively) show that they do contain solid particles, which are the crystalline residues of the dissolution of gum rosin in acetone. The particle size is distributed according to a power law (Figures 1d and 1e), with the deviation for smaller crystal areas at least partly related to the difficulty of counting particles at the resolution limit of an optical microscope (it is also conceivable that the dissolution process is more complete for the smaller particles and that part of the deviation from a power law in Figures 1d and 1e is real). These solid particles may be considered as analogues of crystals in magmas and span in size and number density a relative wide subset of that found for the solid phase in magmatic systems.



Table 1. Densities, Viscosities, and Crystallinities of GRA Mixtures and Acetone^a

Sol (wt %)	Density (kg m ⁻³)	Viscosity (Pa s)	Particle Number Density (mm ⁻²)	Mean Interparticle Distance (mm)
15	1150 ± 50	12.95 ± 0.1		
23	1020 ± 50	0.36 ± 0.02		
30	1000 ± 45	0.0695 ± 0.0013	450	0.03 ± 0.01
35	924 ± 30	0.026 ± 0.005	120	0.04 ± 0.01
40	900 ± 30	0.012 ± 0.001	25	0.1 ± 0.02
Gum rosin	~1100			
Pure acetone	~790	~0.0003		

^aThe uncertainties are representative of the variability of the solutions' characteristics for different stirring time and laboratory temperature. The particle number density and the mean interparticle distance were estimated by counting the particles in the region bordered in white in Figures 1a–1c for 30, 35, and 40 wt % GRA, respectively. A detailed particle size distribution is reported in Figure 1 for a wider set of mixtures and particle dimensions.

The number density of crystals in GRA mixtures and the surface they offer as locus for nucleation are important parameters in this study but impractical to control, because they depend, along with acetone content, laboratory temperature, and pressure, also on the initial size distribution of the crystals provided by the supplier, and on the history of the stirring process. As a result, the solid fraction can vary by up to 1 order of magnitude for the same acetone concentration, or even within the same sample of mixture, as observed in the optical microscope images (Table 1 and Figures 1a–1c), also due to gravitational segregation, which is very efficient for the largest particles. Consequently, we identify the mixtures by their acetone mass content, over which we have a much closer control, remembering the quantity and dimension of the particles is anticorrelated with acetone content in the mixture. This anticorrelation means that we cannot explore a broad range of crystallinity for both low and high acetone content.

[8] If decompressed below the vapor pressure p_B of acetone at the relevant temperature ($p_B = 19.4\text{--}24$ kPa at $15\text{--}20^\circ\text{C}$, see e.g., <http://www.s-oh.com/acetone.html>), GRA mixtures experience acetone bubble nucleation and bubble growth, the mixture expands, and the initial acetone content is reduced to a level depending mainly on the final pressure reached and on the history of decompression [Mourtada-Bonnefoi and Mader, 2004]. GRA mixtures with initial acetone concentration $\sim 15\text{--}30$ wt % have often been used as a laboratory analogue for high-silica magmas in decompression experiments [Phillips et al., 1995; Lane et al., 2001; Blower et al., 2001, 2002; Mourtada-Bonnefoi and Mader, 2004; Stix and Phillips, 2012] because of their large viscosity increase—of several orders of magnitude—on reduction of acetone content (Figure 1f and Table 1; see also Phillips et al. [1995]). Mourtada-

Bonnefoi and Mader [2004] measured reductions of about one third and two thirds of the initial acetone content in decompression experiments resulting in nonexplosive expansion and fragmentation, respectively, which for $15\text{--}25$ wt % GRA mixtures at 18°C (the laboratory temperature during our experiments) corresponds to a viscosity variation from about $0.1\text{--}1$ Pa s to about $10^2\text{--}10^6$ Pa s (and up to 10^{13} Pa s for a stronger volatile depletion). The strong viscosity variation may be at least partially linked to the variation in solid fraction, and in terms of rheology, GRA mixtures might behave as suspensions [Costa et al., 2009; Cimarelli et al., 2011]. The end product is a dry, strong foam similar to pumice. Blower [2001] and Blower et al. [2001, 2002] compared scanning electron microscope (SEM) images of natural pumice and fragmented 20, 25, and 30 wt % GRA samples from fast decompression experiments, documenting polyhedral-shaped bubbles (with vesicularity of about 90%) with a power-law bubble size distribution, which they interpreted as originating from continuous nucleation processes in a highly supersaturated fluid, where slow diffusion limits the growth of nucleated bubbles so that new ones nucleate in the regions of the melt least depleted in volatiles. In this study, we also explored the behavior of $35\text{--}40$ wt % GRA mixtures. Their initial viscosity (of the order of 10^{-2} Pa s, Figure 1f) increases after the experiments to about $10^0\text{--}10^2$ Pa s, and they retain enough acetone during degassing to maintain high mobility and scarce to absent polymerization. The end product of fragmentation is a bubbly liquid mass that becomes more diluted and flows down the glass tube walls when pressure returns to atmospheric and part of the acetone returns into solution. The 30 wt % mixtures show an intermediate behavior (see sections 2.3 and 3.1 for more details). By way of comparison with



initial and degassed viscosities of magmas, we estimate that to match the viscosity of degassed rhyolite and basalt (about $10^8 - 10^9$ Pa s and $10^1 - 10^2$ Pa s, corresponding to 3–5 wt % and 10–13 wt % for our GRA 18°C, respectively), and considering the previously observed reduction to one third of the initial content of GRA mixtures after fragmentation, we require GRA with initial contents of 10–15 wt % and 30–40 wt % acetone, respectively (Figure 1f).

[9] The diffusivity of acetone in 20–30 wt % GRA mixtures at 20°C varies approximately linearly with acetone content from 0.28 to 2.8×10^{-11} m² s⁻¹ [Blower, 2001], which is comparable to the diffusivity of water in basaltic magmas at a temperature of about 900–1100°C and of 700–900°C in rhyolitic magmas, or to the diffusivity of CO₂ at a temperature of 700–900°C in hydrated rhyolitic magmas and of 1200–1400°C in basaltic magmas [Baker *et al.*, 2005]. The surface tension of GRA is in the range 0.028–0.030 J m⁻² [Phillips *et al.*, 1995], higher than the surface tension of pure acetone at our experimental temperatures, which is about 0.023–0.024 J m⁻². However, we observe that macroscopic (>~0.2 mm in radius) gum rosin crystals sinking in the mixtures are the source of continuous bubble nucleation for $p < p_B$ (similar to that documented in Figure 3b, Mourtada-Bonnefoi and Mader [2004], for mustard seeds). These particles have the potential of reducing the effective surface energy in GRA mixtures and promoting bubble nucleation. This effect might be due to the particle shape becoming irregular above a critical particle dimension (see Figure 1a).

[10] In summary, 15–23 wt % GRA mixtures display both the rheological behavior of high-silica magmas during degassing and similar presence of more numerous and vesiculation-effective particles, while 30–40 wt % GRA mixtures behave more similarly to low-silica magmas.

[11] The acetone content in our mixtures leads to an expansion at fragmentation pressure, which can be calculated as follows: the mixtures fragment at or below about 10 kPa. Given that the density of GRAs is about 1000 kg m⁻³ and that the molar mass of acetone is 0.058 g mol⁻¹, 15–40 wt % GRAs contain about 2.5–6.9 moles of acetone per liter of mixture. At fragmentation pressure, if all acetone underwent phase transition (which is an overestimation in particular for slowly decompressed samples), approximating the expansion as isothermal and assuming the ideal gas law, we obtain 600–1600fold expansion.

[12] At final pressure $p_f = 1$ atm and for magma temperatures during eruption in the range 900–1500 K, our mixture expansion will be similar to that of 8–13 moles of gas in 1 L magma, corresponding to a maximum total volatile content of about 5–9 wt % in magma with density 2500 kg m⁻³. Keeping in mind that this represents an overestimation as not all acetone undergoes phase transition instantly and temperature drops during free expansion, this is a relatively large volatile content for low-silica magmas but reasonable for high-silica ones. The large volatile content guarantees that nucleation is not hampered in our experiments by lack of volatiles.

[13] Further information about the magma analogue and additional scaling considerations can be found in section 2.3 and Lane *et al.* [2001].

2.2. Experimental Apparatus and Procedure

[14] The decompression experiments were conducted in a classical shock tube apparatus (Figure 2), consisting of a high-pressure cylindrical shock tube made from a 40 mm (internal diameter) borosilicate glass tube (QVF) connected to a 0.6 m³ steel vacuum chamber via a pneumatically controlled sliding partition with an opening time of about 0.3 s. The vacuum chamber is evacuated by a 40 m³/h oil diffusion vacuum pump (Edwards) and is fitted with a vacuum breaker (Fluid Controls PLC) that can be set to leak atmospheric air into the chamber so that a prescribed linear decompression rate is achieved. For some earlier experiments, a manual leak valve was used in place of the vacuum breaker, with the resulting decompression being only approximately linear.

[15] All experiments started with the GRA mixture at atmospheric pressure p_A (initial pressure $p_i = p_A \approx 10^5$ Pa). We subjected the magma analogue to rapid decompression by first decompressing the vacuum chamber down to a desired final pressure p_f with the partition closed, before opening it rapidly. This created a decompression wave that propagated within the shock tube and decompressed the mixture at about 1 GPa s⁻¹ [see also Spieler *et al.*, 2004]. In contrast, by operating the vacuum pump from the start of the experiment with the partition open and controlling manually the leak valve, or setting the vacuum breaker, air was extracted slowly from the shock tube, and we achieved very slow linear decompression rates (50–400 Pa s⁻¹), significantly lower than those explored in previous GRA studies. A pressure transducer (Edwards active strain gauge) measured the pressure in the vacuum chamber with measurements logged using a National Instruments

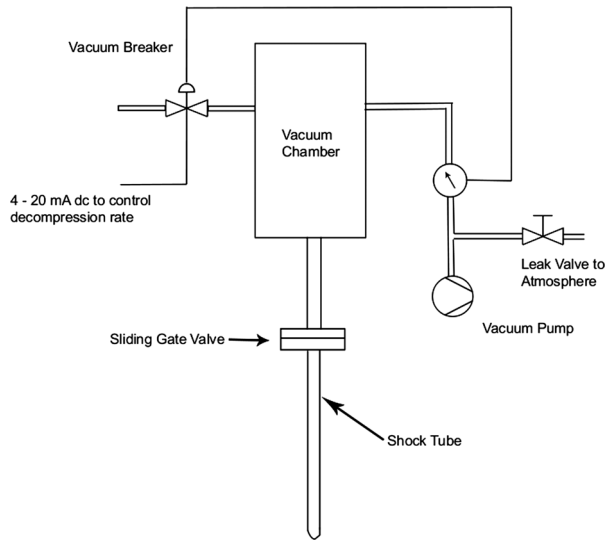


Figure 2. Shock-tube apparatus. A shock tube, containing the sample, is connected to a steel vacuum chamber via a pneumatically controlled sliding partition. The vacuum chamber is evacuated by a vacuum pump and is fitted with a vacuum breaker that can be set to leak atmospheric air into the chamber so that a prescribed linear decompression rate is achieved. An approximately linear decompression rate can also be achieved through a leak valve operated manually. Pressure is measured at three locations: vacuum breaker, between leak valve and vacuum chamber, and within the shock tube.

PCI board. We recorded the experiments using a high-speed video camera (up to 2000 frames/s, Redlake Motionscope) and a conventional video camera (25 frames/s).

2.3. Decompression Rates

[16] The aim of this study was to explore the behavior of magma analogues for decompression rates slow enough that the time scale of decompression is comparable to the time scales of bubble nucleation and bubble growth by diffusion, because the effect of slow decompression on these processes is poorly understood.

[17] Classical theory for homogeneous nucleation predicts the following nucleation rates as a function of supersaturation:

$$J = \frac{2n_0^2 V_m D (\sigma/kT)^{1/2}}{a_0} \exp \left[\frac{-16\pi\sigma^3}{3kT\Delta P^2} \right] \quad (1)$$

where n_0 is the number density of volatile molecules, V_m is the volume of a molecule, D is the volatile diffusivity in the mixture/melt, k is the Boltzmann constant, T is the absolute temperature,

a_0 is the mean distance between volatile molecules, σ is the surface energy, and ΔP is the supersaturation pressure [Toramaru, 1995; Yamada et al., 2005; Mangan and Sisson, 2005]. Employing appropriate values for GRA mixtures ($n_0 = 3.11 \times 10^{27} \text{ m}^{-3}$, $V_m = 1.22 \times 10^{-28} \text{ m}^3$, $a_0 = 6.85 \times 10^{-11} \text{ m}$, and $\Delta P = 20 \text{ kPa}$) yields unrealistically low rates of the order of $\exp(-2.5 \times 10^8) \text{ m}^{-3} \text{ s}^{-1}$. This means that GRA mixtures will require a very long time to nucleation if this occurs homogeneously.

[18] A quantity often used to characterize bubble growth through diffusion in magma is the Peclet number for volatile diffusion [Toramaru, 1995; Gonnermann and Manga, 2007]:

$$Pe_{dif} = \frac{\tau_{dif}}{\tau_{dec}} \quad (2)$$

[19] It describes whether the time scale of diffusion of volatile into bubbles $= (S - R)^2/D$, where S is the distance between bubble centers, R is the bubble radius, and D is the diffusivity, dominates over the time scale of decompression $\tau_{dec} = p_m/(dp/dt)$ (melt pressure divided by decompression rate). If $Pe_{dif} \gg 1$, supersaturation occurs. Assuming that bubbles nucleate immediately on our solid particles ($S - R \sim$ interparticle distance, see Table 1), $\tau_{dif} \sim 30 \text{ s}$ (see Table 1). In our fast decompression experiments, $\tau_{dec} = \sim 10^{-4} \text{ s}$, so that supersaturation is expected. In the slow decompression experiments, $\tau_{dec} = p_B/(dp/dt) \sim 20\text{--}400 \text{ s}$, which is of the same order as τ_{dif} . Hence, for our slowest decompression rates, slow decompression should be accompanied by supersaturation only if at least some of our particles are ineffective as nucleation sites. If the particles are all ineffective as nucleation sites, strong supersaturation is predicted. This is additional evidence for GRA mixtures that have a high acetone content and a low particle content behaving similarly to crystal-poor basaltic magmas during vesiculation, and for GRA mixtures that have a low acetone content but a high particle content behaving similarly to crystal-rich silicic magmas.

3. Experimental Results

3.1. Observations From Fast Decompression Experiments: A Regime Diagram for GRA Mixture Behavior

[20] Upon fast decompression, GRA mixtures show a range of different styles of expansion

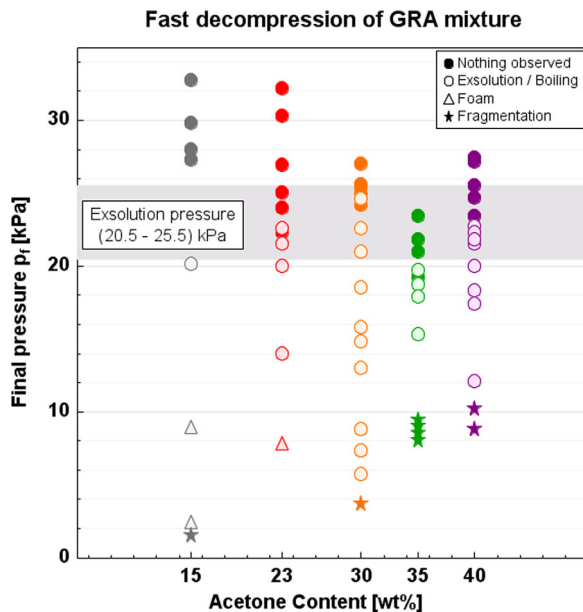


Figure 3. Summary of the results from sudden decompression experiments, showing the phase behavior of the mixture as a function of acetone concentration and total decompression. For $\Delta p > \approx 14 \pm 2$ kPa (hence at a pressure of about 9 ± 2 kPa), mixtures ≥ 35 wt % GRA expand explosively; mixtures ≤ 23 wt % GRA expand significantly but nonexplosively. In order to induce fragmentation in the latter, a decompression of about 21 ± 2 kPa needs to be applied.

depending on acetone content and final pressures p_f (Figure 3):

- (1) Acetone exsolution/bubble nucleation (occurring at 20.5–25.5 kPa across all acetone concentrations): a few bubbles form. They occasionally ascend, and burst at the surface. The mixture does not expand significantly.
- (2) Boiling (occurring at pressures in the range 11–20.5 kPa for all mixture compositions): bubbles form continuously, coalesce, ascend, and burst. The mixture expansion is very small (see movie at http://www.youtube.com/watch?v=VOJiZe_JIHA).
- (3) Foaming (occurring only for 15 and 23 wt % GRA at pressures in the range 1–9 kPa): the mixture rapidly forms bubbles at its surface to create a foam. The mixture/foam column expands at low energy, with velocities of the order of a few cm/s or slower. No fragmentation is observed (the foam does not separate into discrete pieces). Foaming is seen only for low acetone concentrations, because on reduction of acetone content, those mixtures become very viscous and inhibit the movement of bubbles, which become trapped, coalesce,

and expand (see movie at <http://www.youtube.com/watch?v=hGTJHkIBLHo>). For high acetone concentrations, we see vigorous boiling at the same pressure, as more acetone is available in the liquid state to maintain low viscosity and high bubble mobility. Both foaming and vigorous boiling allow different degrees of permeable degassing of the mixtures. The progressive exsolution observed during foaming and vigorous boiling also shows how acetone undergoes phase transition gradually in GRA mixtures, over an extended time period, when below the boiling point.

- (4) Fragmentation (occurring at $p \sim < 1-2$ kPa for GRA ≤ 30 wt % and up to 10 kPa for 35 and 40 wt % GRA): the mixture expands explosively at its surface and fragments. Bubbly pieces separate from the column and are ejected into the vacuum chamber. The column expands at velocities of the order of 1–10 m/s (see movie at http://www.youtube.com/watch?v=U709K_MJQEJ).

3.2. Observations From Slow Decompression Experiments: Evidence for Delayed Nucleation

[21] We performed 34 slow decompression experiments, which show some inherent variability, with very different outcomes following relatively similar decompression histories. A first general result is that we can divide our GRA mixtures into two groups according to their general behavior. GRA mixtures of concentration $< \sim 30$ wt % behave in a fairly uniform and repeatable way; while low-crystallinity 35 and 40 wt % GRA mixtures show the least repeatable results.

[22] We performed three sets of experiments. During the first set, we applied an approximately constant decompression rate and stopped the decompression after the first observation of bubble nucleation or expansion (see Figure 4). While mixtures of concentration ≤ 30 wt % always showed nucleation at pressures 18–25.5 kPa, 35 and 40 wt % concentrated mixtures in some cases did not. In those cases, we continued the decompression, obtaining fragmentation at much lower pressures; within error, at the same value of 7–10 kPa for both 35 and 40 wt % mixtures. During the second set of experiments, we focused on 35 and 40 wt % mixtures. Instead of stopping the decompression after bubble nucleation, we continued the decompression until either fragmentation occurred, or

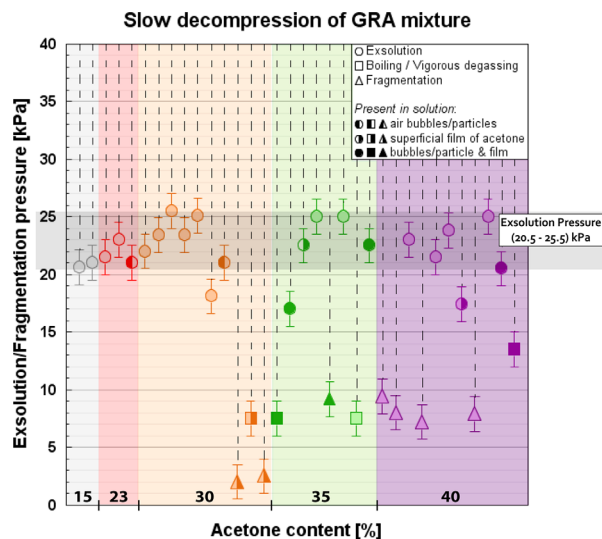


Figure 4. Summary of the results from slow-decompression experiments. All experiments started at atmospheric pressure. The mixture was decompressed at about $100\text{--}400\text{ Pa s}^{-1}$. The typical behavior of the mixtures was to show acetone exsolution in the pressure range $20\text{--}25\text{ kPa}$. Mixtures 30, 35, and 40 wt % sometimes did not display that behavior, and we observed fragmentation at about $7\text{--}10\text{ kPa}$. We always observed nucleation at p_B for $<30\%$ mixtures decompressed slowly.

pressures of about 5 kPa were reached. Sometimes, we observed a few bubbles at pressures greater than 25 kPa , and these were interpreted as air bubbles because the pressure was significantly greater than acetone vapor pressure. When this occurred, we always observed acetone bubble nucleation at pressures $18.0\text{--}25.5\text{ kPa}$ followed by boiling. However, during about half of the experiments, we did not observe any bubbles nucleating at 25 kPa , nor boiling at 20 kPa or at lower pressures. The mixture remained stable and unchanged until pressures of about $7\text{--}10\text{ kPa}$ were reached, and then the mixture fragmented (see Figure 6a and movie at <http://www.youtube.com/watch?v=hoOY9u68yHw>). The fragmentation pressure was approximately the same—within experimental uncertainties—not only for a specific GRA concentration but also across the range of concentrations $35\text{--}40\text{ wt %}$. The fragmentation pressure corresponds to that observed in fast decompression experiments (see Figure 3). The movies reveal the primary mechanism of fragmentation in some of our experiments: no nucleation of bubbles is observed (Figure 5a) until one single bubble appears at the surface (Figure 5b), it expands for a fraction of a second until it is roughly $2\text{--}3\text{ cm}$ in diameter (Figure 5c), then it explodes (Figure 5d)

and triggers fragmentation in the bulk of the mixture through a pressure wave (see horizontal white arrows in Figures 5d–5f, 5i, and 6). The fragmentation proceeds layer by layer [Cashman et al., 2000], with explosive expansion occurring on the surface layer of the mixture (inclined white arrow in Figure 5e), and migrating downward as a “fragmentation layer” (inclined white arrows in Figures 5f–5h) at approximately constant velocity (Figure 5l) as the mixture is ejected upward. Bubble nucleation is a local and unstable process, which becomes global only once energy is transferred to the bulk and periphery of the fluid mass, for example, mechanically through a pressure wave [Cashman et al., 2000]. In our experiments, the surface of the mixture is a favored location for bubble nucleation and expansion; in magma, nucleation occurs internally in the melt with additional expenditure of energy.

[23] In Figure 7a, we display detailed observations from a few significant experiments. The blue curve (Exp J3, 40 wt %) is representative of most of our experiments leading to fragmentation, with no bubble activity whatsoever observed, until the mixture fragments at about 8 kPa . The red and green curves correspond to experiments disrupted by the expansion of air bubbles prior to acetone nucleation. The violet and orange curves correspond to similar decompression rates leading to opposite results: the first one degassed efficiently and did not fragment, while for the second one, we observed bubbles nucleating and later being reabsorbed, and no further nucleation was observed until fragmentation. We interpret this apparent lack of determinism as due to the intrinsic stochasticity of the bubble nucleation process.

[24] We did not observe slow-decompression fragmentation in 30 wt % GRA when decompressed manually. However, if the decompression rate is kept constant electronically using the vacuum breaker (third set of experiments), the same variability (or lack of reproducibility) of results is observed (Figure 7b), except that very low pressures can be reached without any nucleation. When we reached the lowest pressure possible with our equipment without observing any exsolution, we applied a small vibration to the shock tube (the impact of a fingernail at the tube wall) and immediately observed very powerful fragmentation. In other words, it appears that highly localized accelerations (and possibly decelerations) during decompression can stimulate bubble nucleation.

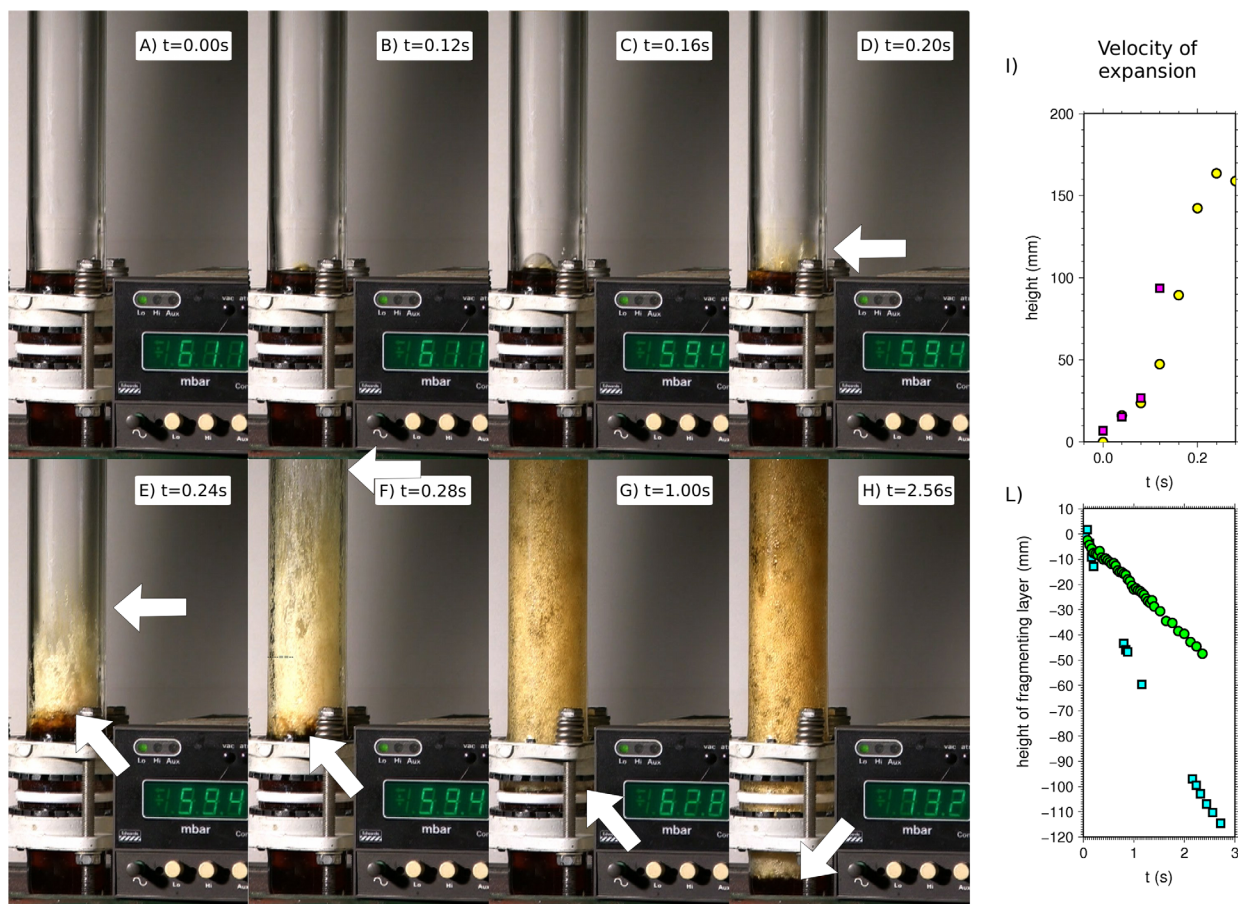


Figure 5. (a–h) Frame-by-frame illustration of fragmentation during slow decompression experiment J3 (40 wt % GRA). Nothing is observed until pressure reaches about 6 kPa or 60 mbar (the display in each image shows the pressure in mbar, for example 61.1 mbar in Figure 5a and 73.2 mbar in Figure 5h). Then, a big bubble appears (arrowed in Figure 5d) and explodes (arrowed in Figure 5e), triggering the fragmentation of the first layer of material. Fragmentation continues on a layer-by-layer fashion (see inclined white arrow indicating the level of the fragmentation layer) until the whole mixture has fragmented. (i) The expansion of the mixture is plotted in pink squares (J3, 40 wt %) and yellow circles (J10, 35 wt %). The velocity of expansion of the ejected fluid is about 0.7–1 m/s, with the mixture having higher volatile content (J3) showing the highest energy expansion, as expected. (j) Downward migration of the fragmentation layer (see bottom of shock tube in Figures 5f–5h) occurring at about 2–5 cm s⁻¹. Light blue squares and green circles mark data from experiments J3 and J10 respectively.

[25] In summary, delayed nucleation, followed by fragmentation, is favored in our experiments if the decompression proceeds at a regular rate, as we observed for a higher percentage of the experiments, and for the 30 wt % mixture, if we used the vacuum breaker.

4. Discussion of the Experimental Results

[26] In some of our slow-decompression experiments, nucleation is retarded until significantly

below the boiling point, even if solid particles are present. Large supersaturation leads to explosive expansion in those cases. We interpret the permeable outgassing of <30 wt % GRA as due to efficient and rapid nucleation, and the occasional explosive expansion of 30, 35, and 40 wt % mixtures as due to supersaturation accompanying a different nucleation mechanism, maybe homogeneous nucleation, maybe heterogeneous and delayed, as discussed below (a review of the physical homogeneous and heterogeneous mechanisms governing bubble nucleation is given by Cashman et al. [2000]).

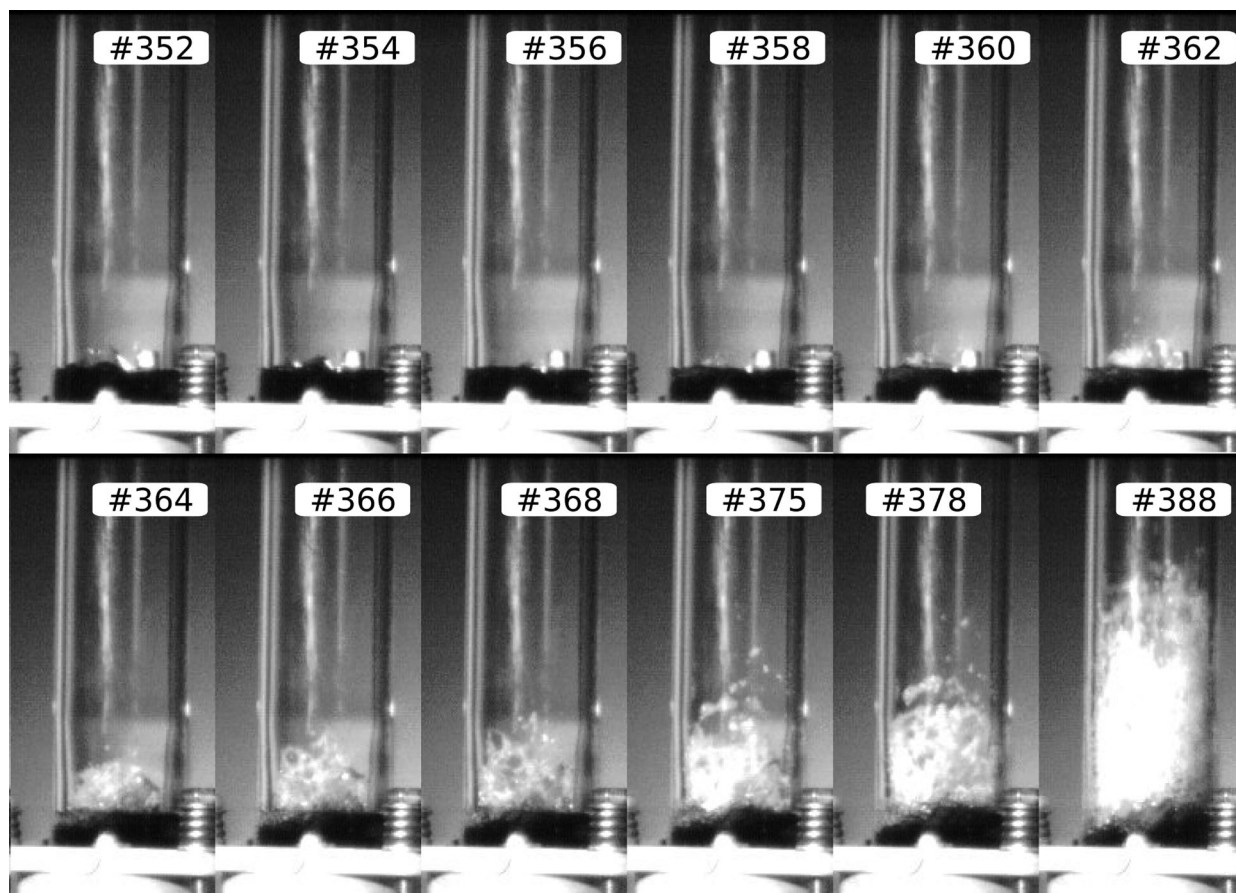


Figure 6. Frames from the high-speed camera movie for experiment J3, recorded at 500 frames/s. The expansion velocity is very high (see Figure 5) but lower than the one observed during fast decompression experiments. In the first frames (352 and 354), a big bubble can be seen to grow and burst. In frame 358 fragmentation starts.

[27] The solid particles of gum rosin contained in our 30, 35, and 40 wt % mixtures seem, in general, to be inefficient nucleation adjuvants, given that we observe nucleation to be delayed. This might arise from a particularly unfavorable wetting angle of acetone bubbles onto gum-rosin solid particles, due to the compositional similarity of the liquid part of GRA mixtures to the particles: the liquid would strongly wet the particles, making them poor substrates for gas nuclei [Mangan *et al.*, 2004]. However, compositional similarity between the liquid and solid phases should be higher for low acetone content, making supersaturation more likely for mixtures low in acetone; this is the contrary of what we observe, as nucleation results to be more efficient for our 23 and 30 wt % mixtures. Higher compositional similarity might be counterbalanced by the availability of more, larger particles, which provide a higher number of nucleation sites or a larger total solid surface as support for nucleation. Therefore, it is

plausible that heterogeneous and efficient nucleation takes place in $< \sim 30$ wt % GRA mixtures (where a great abundance of nucleation sites counterbalances their low efficiency); and either homogeneous nucleation, or heterogeneous but inefficient and delayed nucleation, for $> \sim 30$ wt % GRA mixtures, due to scarce and inefficient nucleation sites. The layer-by-layer explosive expansion we observe during fragmentation is consistent with large supersaturation of the mixture and a nucleation mechanism close to homogeneous [Toramaru, 1995; Cashman *et al.*, 2000], with a pressure wave propagating through the supersaturated fluid triggering progressive mass vesiculation.

[28] Explosive expansion during slow decompression seems to occur at about the same pressure not only for a specific acetone concentration, but for all 30, 35, and 40 wt % GRA, at least for a similar decompression history. The linearity of the

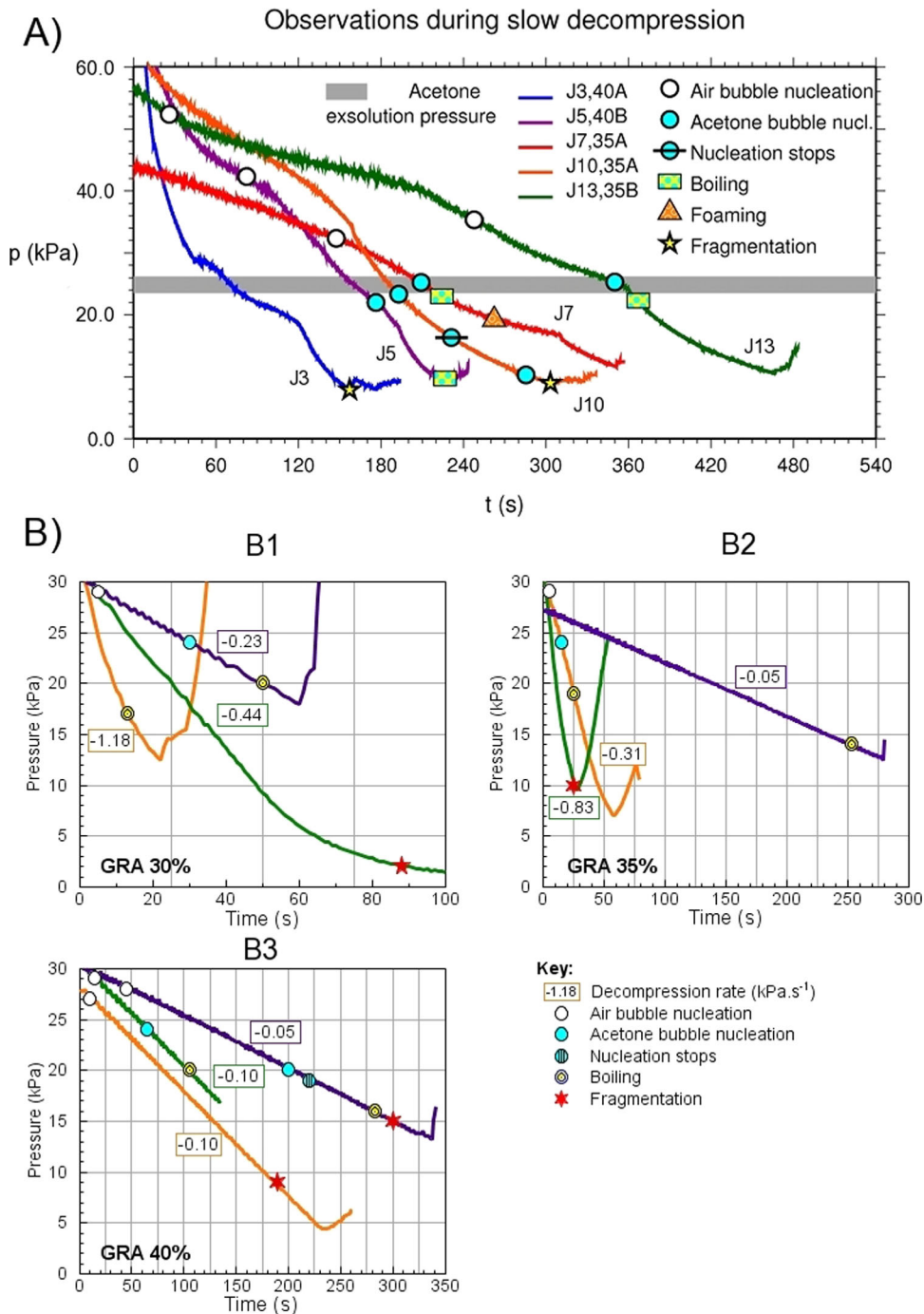


Figure 7. (a) The decompression history during five runs of the experiments is plotted in different colors. The acetone content for the individual runs is indicated in the inlet, along with the description of the symbols used to indicate naked-eye observations at distinct times and corresponding pressures. The blue curve (Exp J3, 40 wt %) is representative of most of our experiments leading to fragmentation. The decompression rate was about 200 Pa s^{-1} in the region of interest ($< 30 \text{ kPa}$) although it was somewhat irregular. We observed no activity until the 40 wt % mixture eventually fragmented at about 8 kPa. The red and green curves in Figure 7a correspond to a decompression rate of about 100 Pa s^{-1} . The expansion of air bubbles prior to acetone nucleation was noted during both of these experiments. The violet and orange curves correspond to similar decompression rates of about $200\text{--}250 \text{ Pa s}^{-1}$ and to a 40 wt % (J5) and 35 wt % (J10) acetone concentration, respectively. The first one degassed efficiently and did not fragment, while for the second one, we observed bubbles nucleating at about 25 kPa, then those bubbles were reabsorbed, and no further nucleation was observed until fragmentation occurred at 7.5 kPa. (b) Decompression history for nine of the slow decompression experiments using solutions with 30% acetone (top-left corner), 35% acetone (top-right corner), and 40% acetone (bottom-left corner). For each experiment, the pressure at which bubbles were observed is indicated, being either air bubbles, acetone exsolution, boiling, or fragmentation. Decompression rates vary between -0.10 and -1.2 kPa s^{-1} . Very low pressures can be obtained without any nucleation by controlling the decompression electronically.

decompression rate (constant rather than accelerated or decelerated) seems to promote delayed nucleation in our experiments over a relatively large range of decompression rates. Our data set does not allow us to resolve any possible dependence of the final fragmentation pressure on acetone concentration. It seems reasonable that this dependence is weak or absent, given that the solubility of acetone does not depend on concentration, and all the acetone becomes potentially available for exsolution immediately below the boiling point of acetone, p_B , so that the amount of supersaturation of the mixture has a dramatic increase as soon as $p < p_B$, but it does not increase much thereafter. Since solubility laws in magma are generally progressive, with more and more volatiles becoming prone to phase change as disequilibrium increases, it is possible that in volcanic systems the difference between saturation pressure and fragmentation pressure does depend on crystallinity or volatile content, as petrology experiments seem to confirm (see section 4.3). However, if the conditions are similar, our experiments indicate that fragmentation will be induced by a specific pressure differential. A regular decompression at approximately constant rate, such as that due to lava flow reducing pressure on the magmatic system below, causing magma to ascend slowly and unperturbed in the conduit (rather than convecting and mixing continuously) could be a promoting factor for delayed bubble nucleation.

4.1. Comparison With Decompression Experiments on Rhyolitic Magmas

[29] Bubble nucleation has been studied mostly in rhyolitic melts, to which most explosive eruptions are linked. In the last few years, a growing weight of evidence has suggested delayed bubble nucleation as a viable mechanism of explosive expansion of high-silica magmas.

[30] Mangan and Sisson [2000] decompressed rhyolite that had been remelted until crystal free, in order to reach the conditions for homogeneous nucleation. They observed large supersaturation and noted that the pressure differential needed to nucleate bubbles depended on the mechanism of bubble nucleation (homogeneous, heterogeneous, or a combination of them). At a given decompression rate, they found that the abundance of nucleation-facilitating crystals controls degassing efficiency and the likelihood of strong supersaturation. They conclude that homogeneous nucleation tends to occur even in relatively crystalline rhyo-

lites, containing up to 10^6 crystals cm^{-3} . Our observations and interpretation of delayed bubble nucleation in our experiments are compatible with a similar mechanism. More observations are required to prove and constrain a relationship between decompression rate and critical crystallinity for analogue experiments.

[31] *Mourtada-Bonnefoi and Laporte* [2002] showed that magma can reach high levels of supersaturation depending on gas content and crystallinity. The results of their decompression experiments are that a smaller difference between saturation pressure and bubble nucleation pressure (60–160 MPa) is observed at high content of H_2O ($\sim 7\%$), while if the content in water is lower ($< 5\%$) and crystallinity is low, very high levels of supersaturation (135–310 MPa) may be reached in the magma before nucleation occurs, sometimes explosively. Once started, the nucleation occurs in seconds to minutes. As mentioned above, in our experiments the solubility curve is roughly the same for the 30, 35, and 40 wt % GRA, which might be the reason why we observe the same supersaturation level Δp in all our fragmentation events, at least for a similar decompression history.

[32] *Iacono Marziano et al.* [2007] decompressed at varying rates K-phonolitic magmas from the Vesuvius AD 79 eruption and found that slow decompression rates (2.8, 24, and 170 kPa s^{-1}) lead to bubble nucleation at the capsule-melt interface. They calculate surface tension values of about 0.095 J m^{-2} , more similar to values for rhyolite than dacite. They conclude that decompression rates and magma crystallinity control the bubble nucleation mechanism. They infer that delayed disequilibrium degassing may have played a crucial role in that eruption.

4.2. Application to Basaltic Magmas

[33] While there is a relative abundance of published decompression experiments on remelted and rehydrated rhyolite samples and in general on high-silica magmas, no slow decompression experiments on basalts have been published to date, hindering possible comparisons between our results and petrological experiments, as well as direct links with basaltic volcanoes. Necessarily, our application to basaltic volcanic systems will be mainly of speculative character.

[34] In general, delayed bubble nucleation has been thought unlikely for low-silica melts, because they have larger diffusivity [*Pinkerton et al.*,

2002] and a lower surface energy and hence a lower barrier to nucleation than high-silica melts, so that bubbles tend to form early during ascent and volatiles tend to exsolve efficiently [Mangan *et al.*, 2004]. On the other hand, the presence of crystals in basaltic magma has a smaller disruptive power than for high-silica magmas: network-modifying cations and dissolved volatile molecules are very efficient in disrupting the strongly linked framework of highly polymerized melts, but less so in low-silica compositions [Mangan and Sisson, 2005]. The wetting angle of bubbles onto the same type of crystals is larger for high-silica magmas than for low-silica magmas, where it is small (but nonzero, as bubbles still tend nucleate on crystals; see e.g. Figure 2 in Mangan *et al.* [2004]). Hence, the distinction between homogeneous and heterogeneous nucleation becomes blurred for such less polymerized, low-silica magmas, as Mangan and Sisson [2005] demonstrated for dacite as opposed to rhyolite. Therefore, it seems reasonable that the nucleation-facilitating effects of a low-energy barrier to nucleation in low-silica magmas could be compensated by a diminished efficiency of crystals in supporting nucleation, making delayed bubble nucleation a viable mechanism for high-energy explosive eruptions of volatile-rich, poorly crystalline basalts. Our experimental results, where delayed bubble nucleation and mass vesiculation occurred more frequently on low-viscosity magma analogues, with a molecular structure that does not tend to polymerize such as that of GRA with high acetone content, support this argument. Experimental data for basalts are needed in order to confirm or exclude this hypothesis.

4.3. Comparison With Published Experimental Studies on Slow Decompression of Magma Analogues

[35] Analogue experiments on the effects of decompression rate may be divided into two categories: those that use volatile-bearing fluids as the magma analogue, where bubble nucleation takes place during the experiments [e.g., Phillips *et al.*, 1995; Lane *et al.*, 2001; Stix and Phillips, 2012], and those that use bubbly fluids, where preexisting bubbles are introduced into the fluid before the experiment starts [e.g., Namiki and Manga, 2006]. None of the published experiments of either type has evidenced any explosive behavior during decompressions as slow as in our experiments. We now compare our observations with those from previous studies.

[36] If decompressed at slow decompression rates in the laboratory, bubbly fluids expand with various nonexplosive styles [Namiki and Manga, 2006], which we also observe when nucleation is efficient, and describe generically as “foaming.” Since we find that bubble nucleation (not studied in those experiments, which involved preexisting bubbles) controls fragmentation during slow decompression, our experiments complement previous findings, rather than conflicting with them. However, Namiki and Manga [2006] find that the height of the bubbly column is an important parameter for the outcome of slow decompression; they suggest from theoretical arguments that if the bubbly column in a volcanic conduit reaches height > 1 km, then decompression rates typical of lava effusion ($10^2 - 10^3$ Pa s⁻¹) may lead low viscosity magma to nonequilibrium expansion. It is challenging to compare that theory with our observations as we do not know how much of the initial acetone exsolves, and at what rate, during expansion. Nucleation has been in fact observed to take place progressively in GRA mixtures, as happens for magma undergoing sudden decompression [Blower *et al.*, 2001, 2002].

[37] Stix and Phillips [2012] decompressed GRA mixtures at very slow rates (down to 20–80 Pa s⁻¹), in apparatus similar to ours but with acetone concentration in the range 15–30 wt %. They observed different degassing styles at different pressures but no fragmentation in any of the experiments. However, they did not explore 35 and 40 wt % mixtures, which are the ones in which we observe fragmentation if decompressed at those rates. Also, they did not apply a constant decompression rate either manually or with a vacuum breaker, and their decompression rate was not constant but decreased with time.

[38] Air bubbles present in our mixtures seem to suppress supersaturation and favor diffuse nucleation, probably because these air bubbles represent stable nuclei of gas accumulation and, by growing, they release free energy. This is consistent with results from Mourtada-Bonnefoi and Mader [2004], who also used GRA mixtures and found that nucleation is very efficient if solid particles of various materials are present in a magma analogue. In the light of our results, those experiments did not observe any large deviation from equilibrium, probably because the particles added to those GRA mixtures were efficient nucleation sites or were trapping tiny air bubbles, or just because in those experiments < 30 wt % GRA mixtures were used.

[39] Additional analogue experiments could be designed in order to improve the similarity to magma, for example, it could be attempted to dissolve two different volatile species into gum rosin, in order to check whether the resulting solubility law is more progressive. In order to clarify the nucleation dynamics in GRA solutions, experiments could also be designed to explore in detail the properties of GRA mixtures, for example, surface energy and wetting angles. Also, it would be desirable to measure the wetting angle of acetone bubbles on gum-rosin particles immersed in fluid GRA mixtures [see, e.g., *Mangan et al.*, 2004]. This requires microscope images of the mixture at the exsolution pressure of acetone (20–25 kPa), as acetone is liquid if pressure is atmospheric. An experiment could also be designed to study the end products of fragmentation during slow-decompression versus foaming resulting from efficient nucleation and degassing.

5. Formulation of a Conceptual Model of Delayed Bubble Nucleation in Low-Silica Volcanic Systems

[40] In summary, our analogue experiments suggest that the idea that crystal-poor low-silica magma, carrying insufficient and inefficient bubble nucleation sites, may build up large supersaturation if slowly decompressed, should be further investigated.

[41] We propose the following conceptual model of delayed, nonequilibrium degassing of a high- and low-silica volcano as a possible explanation for a sudden change in the eruptive regime, from effusive to explosive. During effusive activity, the magma ascending in the conduits is decompressed at a slow rate, and volatile-rich, crystal-poor magma will feed the conduits from below. With slow ascent rates, the flow will have low Reynolds numbers even for low viscosities, so that no turbulent mixing can promote bubble nucleation. If crystallinity is very low and if the crystals present are of the nucleation-inefficient types, the ascending magma may undergo delayed nucleation, supersaturating progressively and becoming increasingly metastable. Magma could supersaturate even in presence of exsolved bubbles, provided their number density is small and the magma is not sufficiently depleted in volatiles through diffusion. Mass vesiculation is triggered either when this magma batch reaches a specific Δp (which could correspond to reaching a specific level in the plumbing system) or when it

reaches a specific location where its periphery comes into contact with stored magma with a high crystal content, for example, in a shallow reservoir. This contact may induce bubble nucleation at the periphery of the magma batch, be rapidly transmitted as a pressure wave throughout the whole volume of supersaturated magma, and cause an explosive expansion of the magma column in volatile-coupled conditions. The explosive expansion may be accompanied or followed by mass crystallization, due to a sudden drop of the liquidus temperature [*Hort*, 1998]. The fragmentation surface propagates downward, layer by layer, until the batch of supersaturated magma is exhausted. The power of the explosive expansion depends on the level of supersaturation Δp and on the volatile content. The duration of the explosive expansion depends on the mass or height of column of supersaturated magma available and on the geometry of the plumbing system (the total energy will depend on the three factors). The reason why explosive basaltic eruptions are observed only episodically may ultimately result from the low likelihood of many simultaneous conditions that need to be satisfied for the mechanism to occur.

[42] We expect this mechanism to be generally relatively short lived and isolated (once the magma batch is exhausted or the reservoir is empty, the explosive expansion ceases, and before a new explosive eruption occurs, the system needs first to regain stability and to accumulate volatile-rich magma, and then to undergo slow decompression) and to produce materials tapped directly from deeper reservoirs. This is consistent to what observed during the last 10 years of close observation at Stromboli, where the usual mildly explosive activity is associated with high porphyritic magma from the upper reservoir, containing nucleation-facilitating crystals such as titanium and iron oxides, and where paroxysms, and to some extent major explosions, are associated with low porphyritic blond magma from a deep reservoir, where nucleation-facilitating crystals are not found [e.g., *Métrich et al.*, 2001; *Pichavant et al.*, 2009].

[43] Earthquakes or any other form of pressure wave shaking supersaturated basaltic magma stored in conduits may also trigger delayed nucleation (similar to the explosive expansion of our supersaturated mixture resulting from the impact of a fingernail on the shock tube); if this occurs, the intensity of the response of the magmatic system should depend on the degree of supersaturation reached.

[44] In the case of sudden decompression, mass vesiculation and crystallization occur releasing at once the energy provided by the decompression, while in case of slow decompression, the energy is stored slowly in the magma and released later in a short time interval as a cascade effect.

6. Conclusions

[45] The conceptual model presented here is consistent with the physics of phase transition in multicomponent mixtures and compatible with observations from published results on decompression of remelted magma samples. It offers a possible explanation for high-energy low-silica explosive eruptions, which remain unexplained. Although petrological studies are required to demonstrate that delayed bubble nucleation followed by explosive expansion can really apply to basaltic systems in general and specifically to a given eruptions at a given volcano, this model suggests that decompression due to lava effusion, which is generally considered a low-risk eruptive style, can potentially trigger powerful explosive eruptions. The eruption process would actually be triggered when decompression starts, but an explosive eruption would only occur when sufficient magma has spilled from the conduit [Calvari et al., 2011], that the pressure drop exceeds that capable of being sustained by delayed nucleation, with the extruded magma volume being a proxy for the pressure differential Δp required for fragmentation.

Acknowledgments

[46] F. Maccaferri, S. Paillat, C. Cimarelli, and various students from the Geological Fluid Dynamics Laboratory in the School of Earth Sciences, University of Bristol, helped during the experiments. Dan Morgan helped with the quantification of crystallinity. Discussion with S. Lane and J. Neuberg and insightful comments by M. Mangan and two anonymous reviewers helped improving the manuscript. This project was funded by the Italian Civil Defense Agency and the Istituto Nazionale di Geofisica e Vulcanologia (project INGV-DPC Paroxysm V2/03, 2007–2009) and by an ERC Starting Grant (project CCMP-POMPEI). Logistic support by Cen/DTU (Denmark) is gratefully acknowledged.

References

Aiuppa, A., M. Burton, P. Allard, T. Caltabiano, G. Giudice, S. Gurrieri, M. Liuzzo, and G. Salerno (2011), First observational evidence for the CO₂-driven origin of Stromboli's

- major explosions, *Solid Earth*, 2, 135–142, doi:10.5194/se-2-135-2011.
- Baker, D., C. Freda, R. A. Brooker, and P. Scarlato (2005), Volatile diffusion in silicate melts and its effects on melt inclusions, *Ann. Geophys.*, 48(4/5), 699–717.
- Blower, J. D. (2001), Degassing processes in volcanic eruptions, PhD thesis, Univ. of Bristol, Bristol, U. K.
- Blower, J. D., J. P. Keating, H. M. Mader, and J. C. Phillips (2001), Inferring volcanic degassing processes from vesicle size distributions, *Geophys. Res. Lett.*, 28(2), 347–350.
- Blower, J. D., J. P. Keating, H. M. Mader, and J. C. Phillips (2002), The evolution of bubble size distributions in volcanic eruptions, *J. Volcanol. Geotherm. Res.*, 1(20), 1–23.
- Calvari, S., L. Spampinato, A. Bonaccorso, C. Oppenheimer, E. Rivalta, and E. Boschi (2011), Lava effusion—A slow fuse for paroxysms at Stromboli volcano?, *Earth Planet. Sci. Lett.*, 301(1-2), 317–323, doi:10.1016/j.epsl.2010.11.015.
- Cashman, K. V., B. Sturtevant, P. Papale, and O. Navon (2000), *Magmatic fragmentation*, in *Encyclopedia of Volcanoes*, edited by H. Sigurdsson, pp. 421–430, Academic, San Diego, Calif.
- Castro, J. M., and J. E. Gardner (2008), Did magma ascent rate control the explosive-effusive transition at the Inyo volcanic chain, California?, *Geology*, 36, 279–282.
- Cervantes, P., and P. Wallace (2003), Magma degassing and basaltic eruption styles: A case study of ~2000 year BP Xitle volcano in central Mexico, *J. Volcanol. Geotherm. Res.*, 120(3-4), 249–270.
- Cimarelli, C., A. Costa, S. Mueller, and H. M. Mader (2011), Rheology of magmas with bimodal crystal size and shape distributions: Insights from analog experiments, *Geochem. Geophys. Geosyst.*, 12, Q07024, doi:10.1029/2011GC003606.
- Coltelli, M., P. Del Carlo, and M. Vezzoli (1998), Discovery of a Plinian basaltic eruption of Roman age at Etna volcano, Italy, *Geology*, 26(12), 1095–1098.
- Costa, A., L. Caricchi, and N. Bagdassarov (2009), A model for the rheology of particle-bearing suspensions and partially molten rocks, *Geochem. Geophys. Geosyst.*, 10, Q03010, doi:10.1029/2008GC002138.
- Doubik, P., and B. E. Hill (1999), Magmatic and hydromagmatic conduit development during the 1975 Tolbachik eruption, Kamchatka, with implications for hazard assessment at Yucca Mountain, NV, *J. Volcanol. Geotherm. Res.*, 91, 43–64.
- Fiebach, K., and D. Grimm (2000), Resins, natural, in *Ullmann's Encyclopedia of Industrial Chemistry*, Wiley-VCH Verlag, doi:10.1002/14356007.a23_073.
- Gonnermann, H. G., and M. Manga (2007), The fluid mechanics inside a volcano, *Annu. Rev. Fluid Mech.*, 39, 321–56.
- Gurenko, A. A., A. B. Belousov, R. B. Trumbull, and A. V. Sobolev (2005), Explosive basaltic volcanism of the Chikurachki Volcano (Kurile arc, Russia): Insights on pre-eruptive magmatic conditions and volatile budget revealed from phenocryst-hosted melt inclusions and groundmass glasses, *J. Volcanol. Geotherm. Res.*, 147, 203–232.
- Gurioli, L., A. J. L. Harris, B. F. Houghton, M. Polacci, and M. Ripepe (2008), Textural and geophysical investigation of explosive basaltic activity at Villarrica volcano, *J. Geophys. Res.*, 112, B05213. Doi: 10.1029/2007JB005328.
- Höskuldsson, À., N. Óskarsson, R. Pedersen, K. Grönvold, K. Vogfjörð, and R. Ólafsdóttir (2007), The millennium eruption of Hekla in February 2000, *Bull. Volcanol.*, 70, 169–182.

- Houghton, B. F., and Gonnerman, H. M. (2008), Basaltic explosive volcanism: Constraints from deposits and models, *Chem. Erde*, *68*, 117–140.
- Hort, M. (1998), Abrupt change in magma liquidus temperature because of volatile loss or magma mixing: Effects on nucleation, crystal growth and thermal history of the magma, *J. Petrol.*, *39*(5), 1063–1076.
- Hurwitz, S., and O. Navon (1994), Bubble nucleation in rhyolitic melts: Experiments at high pressure, temperature and water content, *Earth Planet. Sci. Lett.*, *122*, 267–280.
- Iacono Marziano, G., B. C. Schmidt, and D. Dolfi (2007), Equilibrium and disequilibrium degassing of a phonolitic melt (Vesuvius AD 79 “white pumice”) simulated by decompression experiments, *J. Volcanol. Geotherm. Res.*, *161*, 151–164.
- Krauskopf, K. B. (1948), Mechanism of eruption at Parícutin Volcano, Mexico. *Bull. Geol. Soc. Am.*, *69*, 711–732.
- Lane, S. J., B. A. Chouet, J. C. Phillips, P. Dawson, G. A. Ryan, and E. Hurst (2001), Experimental observations of pressure oscillations and flow regimes in an analogue volcanic system, *J. Geophys. Res.*, *106*, 6461–6476.
- Larsen, J. F. (2008), Heterogeneous bubble nucleation and disequilibrium H₂O exsolution in Vesuvius K-phonolite melts, *J. Volcanol. Geotherm. Res.*, *175*(3), 278–288.
- Mangan, M., and T. Sisson (2000), Delayed, disequilibrium degassing in rhyolite magma: Decompression experiments and implications for explosive volcanism, *Earth Planet. Sci. Lett.*, *183*(3–4), 441–455.
- Mangan, M., T. Sisson, and W. B. Hankins (2004), Decompression experiments identify kinetic controls on explosive silicic eruptions, *Geophys. Res. Lett.*, *31*, L08605, doi:10.1029/2004GL019509.
- Mangan, M. and T. Sisson (2005), Evolution of melt-vapor surface tension in silicic volcanic systems: Experiments with hydrous melts, *J. Geophys. Res.*, *110*, B01202, doi:10.1029/2004JB003215.
- Métrich, N., A. Bertagnini, P. Landi, and M. Rosi (2001), Crystallization driven by decompression and water loss at Stromboli volcano (Aeolian Islands, Italy), *J. Petrol.*, *42*, 1471–1490.
- Métrich, N., A. Bertagnini, and A. Di Muro (2009), Conditions of magma storage, degassing and ascent at Stromboli: New insights into the volcano plumbing system with inferences on the eruptive dynamics, *J. Petrol.*, *51*(3), 603–626.
- Mourtada-Bonnefoi, C., and D. Laporte (2002), Homogeneous bubble nucleation in rhyolitic magmas: An experimental study of the effect of H₂O and CO₂, *J. Geophys. Res.*, *107*(B4), 2066, 10.1029/2001JB000290.
- Mourtada-Bonnefoi, C. C., and H. M. Mader (2004), Experimental observations of the effect of crystals and pre-existing bubbles on the dynamics and fragmentation of vesiculating flows, *J. Volcanol. Geotherm. Res.*, *129*(1–3), 83–97.
- Namiki, A., and M. Manga (2005), Response of a bubble bearing viscoelastic fluid to rapid decompression: Implications for explosive volcanic eruptions, *Earth Planet. Sci. Lett.*, *236*, 269–284.
- Namiki, A., and M. Manga (2006), Influence of decompression rate on the expansion velocity and expansion style of bubbly fluids, *J. Geophys. Res.*, *111*, B11208, doi:10.1029/2005JB004132.
- Namiki, A., and M. Manga (2008), Transition between fragmentation and permeable outgassing of low viscosity magmas, *J. Volcanol. Geotherm. Res.*, *169*, 48–60.
- Parfitt, E. A., and L. Wilson (1995), Explosive volcanic eruptions. The transition between Hawaiian-style lava fountain-
ing and Strombolian explosive activity, *Geophys. J. Int.*, *121*, 226–232.
- Phillips, J. C., S. J. Lane, A. M. Lejeune, and M. Hilton (1995), Gum rosin–acetone system as an analogue to the degassing behaviour of hydrated magmas, *Bull. Volcanol.*, *57*, 263–268.
- Pichavant, M., I. Di Carlo, Y. Le Gac, S. Rotolo, and B. Scaillet (2009), Experimental constraints on the deep magma feeding system at Stromboli Volcano, Italy, *J. Petrol.*, *50*, 601–624.
- Pinkerton, H., L. Wilson, and R. Macdonald (2002), The transport and eruption of magma from volcanoes: A review, *Contemp. Phys.*, *43*(3), 197–210.
- Polacci, M., P. Papale, and M. Rosi (2001), Textural heterogeneities in pumices from the climactic eruption of Mount Pinatubo, 15 June 1991, and implications for magma ascent dynamics, *Bull. Volcanol.*, *63*, 83–97.
- Polacci, M., L. Pioli, and M. Rosi (2003), The Plinian phase of the Campanian Ignimbrite eruption (Phlegrean Fields, Italy): Evidence from density measurements and textural characterization of pumice, *Bull. Volcanol.*, *65*, 418–432.
- Polacci, M., D. R. Baker, L. Mancini, G. Tromba, and F. Zanini (2006), Three-dimensional investigation of volcanic textures by X-ray microtomography and implications for conduit processes, *Geophys. Res. Lett.* *33*, L13312, doi:10.1029/2006GL026241.
- Ryan, G. (2001), The flow of rapidly decompressed gum rosin di-ethyl ether and implications for volcanic eruption mechanisms, PhD thesis, Lancaster Univ., Lancaster, U. K.
- Sable, J. E., B. F. Houghton, P. Del Carlo, and M. Coltelli (2006), Changing conditions of magma ascent and fragmentation during the Etna 122 BC basaltic Plinian eruption: Evidence from clast microtextures, *J. Volcanol. Geotherm. Res.*, *158*, 333–354.
- Sable, J. E., B. F. Houghton, C. J. N. Wilson, and R. J. Carey (2009), Eruption mechanisms during the climax of the Tarawera 1886 basaltic Plinian eruption inferred from microtextural characteristics of the deposits, in *Studies in Volcanology: The Legacy of George Walker*, Spec. Publ. IAVCEI, vol. 2, edited by T. Thordarson et al., pp. 129–154, Geol. Soc., London.
- Schipper, C. I., J. D. L. White, B. F. Houghton, N. Shimizu, and R. B. Stewart (2010), Explosive submarine eruptions driven by volatile-coupled degassing at Loihi Seamount, Hawai’i, *Earth Planet. Sci. Lett.*, *295*, 497–510.
- Shaw, H. R. (1972), Viscosities of magmatic silicate liquids: An empirical method of prediction, *Am. J. Sci.*, *272*, 870–893.
- Sparks, S. (1978), The dynamics of bubble formation and growth in magmas: A review and analysis, *J. Volcanol. Geotherm. Res.*, *3*, 1–37.
- Spieler, O., B. Kennedy, U. Kueppers, D. B. Dingwell, B. Scheu, and J. Taddeucci (2004), The fragmentation threshold of pyroclastic rocks, *Earth Planet. Sci. Lett.*, *226*(1–2), 139–148.
- Stix, J., and J. Phillips (2012), An analog investigation of magma fragmentation and degassing: Effects of pressure, volatile content, and decompression rate, *J. Volcanol. Geotherm. Res.*, *211–212*, 12–23.
- Toramaru, A. (1995), Numerical study of nucleation and growth of bubbles in viscous magmas, *J. Geophys. Res.*, *100*(B2), 1913–1931.
- Vergnolle, S., and C. Jaupart (1986), Separated two-phase flow and basaltic eruptions, *J. Geophys. Res.*, *91*(B12), 12,842–12,860, doi:10.1029/JB091iB12p12842.



Vergnolle, S., and M. Mangan (2000), *Hawaiian and Strombolian Eruptions*, in *Encyclopedia of Volcanoes*, edited by H. Sigurdsson, pp. 447–461, Academic, San Diego, Calif.

Walker, G. P. L., S. Self, and L. Wilson (1984), Tarawera 1886, New Zealand—A basaltic plinian fissure eruption, *J. Volcanol. Geotherm. Res.*, *21*, 61–78.

Williams, S. N., and S. Self (1983), The October 1902 Plinian eruption of Santa Maria volcano, Guatemala, *J. Volcanol. Geotherm. Res.*, *16*, 33–56.

Yamada, K., H. Tanaka, K. Nakazawa, and H. Emori (2005), A new theory of bubble formation in magma, *J. Geophys. Res.*, *110*, B02203, doi:10.1029/2004JB003113.